

New High Precision Measurement of the Reaction Rate of the $^{18}\text{O}(p, \alpha)^{15}\text{N}$ Reaction via THM

M. La Cognata^{A,B}, C. Spitaleri^{A,B,C}, A.M. Mukhamedzhanov^D, B. Irgaziev^E, R.E. Tribble^D, A. Banu^D, S. Cherubini^{A,B}, A. Coc^F, V. Crucillà^{A,B}, V.Z. Goldberg^D, M. Gulino^{A,B}, G.G. Kiss^G, L. Lamia^{A,B}, Li Chengbo^{A,H}, J. Mrazek^G, R.G. Pizzone^{A,B}, S.M.R. Puglia^{A,B}, G.G. Rapisarda^{A,B}, S. Romano^{A,B}, M.L. Sergi^{A,B}, G. Tabacaru^D, L. Trache^D, W. Trzaska^I and A. Tumino^{A,B}

^A INFN - Laboratori Nazionali del Sud, Catania, Italy

^B DMFCI Università di Catania, Catania, Italy

^D Cyclotron Institute Texas A&M University, College Station (TX), USA

^E GIK Institute of Engineering Sciences and Technology, Topi District, Swabi, Pakistan

^F CSNSM CNRS/IN2P3 Université Paris Sud, Orsay, France

^F ATOMKI, Debrecen, Hungary

^G Nuclear Physics Institute of ASCR, Rez near Prague, Czech Republic

^H China Institute of Atomic Energy, Beijing, China

^I Physics Department, University of Jyväskylä, Finland

^C Email: Spitaleri@lns.infn.it

Abstract: The $^{18}\text{O}(p, \alpha)^{15}\text{N}$ reaction rate has been extracted by means of the Trojan horse method. For the first time the contribution of the 20 keV peak has been directly evaluated, giving a value about 35% larger than previously estimated. The present approach has allowed to improve the accuracy of a factor 8.5, as it is based on the measured strength instead of educated guesses or spectroscopic measurements. The contribution of the 90 keV resonance has been determined as well, which turned out to be of negligible importance to astrophysics.

Keywords: Write keywords here

1 Astrophysical motivations

Fluorine is one of the few elements whose nucleosynthesis is still uncertain. Three possible astrophysical factories for fluorine production have been identified, namely Type II Supernovae (SNe II), Wolf-Rayet (WR) stars, and asymptotic giant branch (AGB) stars (Renda et al. 2004). As regards AGB stars, which represents the final nucleosynthetic phase in low and intermediate mass stars, spectroscopic observations have shown that in giant stars of type K, M, MS, S, SC, and C fluorine abundance is enhanced with respect to the solar by up to a factor 30 (Jorissen, Smith, & Lambert 1992). Thus low-mass evolved stars are observationally confirmed astrophysical sites where fluorine is produced. Inside AGB stars, ^{19}F nucleosynthesis takes place at the same evolutionary stage and in the same region as the s-process nucleosynthesis, which represents the nuclear process leading to the generation of heavy elements along the stability valley. For these reason AGB stars play an extremely important role in astrophysics and the understanding of fluorine production, allowing to constrain the existing models (Lugaro et al. 2004), would make predictions on AGB star nucleosynthesis and s-process element yields more accurate. In detail, ^{19}F is produced during the thermal pulse that is

ignited in the ^4He -rich intershell region of AGB stars, following the ingestion of the ^{13}C pocket. The subsequent third dredge-up (TDU) episode mixes the products of shell flash He-burning (thermal pulse), including fluorine, and s-process nuclei to the outer layers. Because ^{19}F abundance is very sensitive to the temperatures and the mixing processes taking place inside AGB stars, it constitutes a key parameter to constrain AGB star models (Lugaro et al. 2004). Anyway, if standard theoretical abundances are compared to the observed ones (Jorissen, Smith, & Lambert 1992), a remarkable discrepancy shows up because the largest ^{19}F abundances cannot be matched for the typical $^{12}\text{C}/^{16}\text{O}$ ratios (Lugaro et al. 2004). It has been shown that extra-mixing phenomena, such as the cool bottom process (Nollett, Busso, & Wasserburg 2003), could help to pin down the origin of this discrepancy (Lugaro et al. 2004).

A complementary way to explain ^{19}F abundance can be provided by nuclear physics, in particular by an improved measurement of the $^{18}\text{O}(p, \alpha)^{15}\text{N}$ reaction rate. In fact this reaction represents the main ^{15}N production channel, which is burnt to ^{19}F via the $^{15}\text{N}(\alpha, \gamma)^{19}\text{F}$ reaction during thermal pulses, at temperatures of the order of 10^8 K. Thus a larger $^{18}\text{O}(p, \alpha)^{15}\text{N}$ reaction rate would lead to an increase

of the ^{19}F supply, while the $^{12}\text{C}/^{16}\text{O}$ ratio would not change. Such an alternative account would also imply an enrichment of ^{15}N in the stellar surface, as a result of the cool bottom processing of material from AGB outer layers at the bottom of the convective envelope (Nollett, Busso, & Wasserburg 2003), at temperatures of about 10^7 K. Therefore a new investigation of the $^{18}\text{O}(p, \alpha)^{15}\text{N}$ reaction at low energies, in the 0-1 MeV energy range would also play a key role to explain the long-standing problem of the $^{14}\text{N}/^{15}\text{N}$ ratio in meteorite grains (Nollett, Busso, & Wasserburg (2003) and references therein) besides the ^{19}F yield. Indeed this ratio turns out to be much smaller than the predicted one for mainstream and A+B grains and any proposed astrophysical explanation, including extra-mixing scenarios, could not help to make the model predictions more accurate (Nollett, Busso, & Wasserburg 2003). In the following the first measurement of the low-laying resonances in the $^{18}\text{O}(p, \alpha)^{15}\text{N}$ reaction is discussed and how the reaction rate is influenced is extensively illustrated.

2 Current status

In the 0-1 MeV energy range, which is the most relevant to astrophysics, 9 resonances show up in the $^{18}\text{O}(p, \alpha)^{15}\text{N}$ cross section. Among these, the 20 keV, 144 keV and the 656 keV resonances determine the reaction rate (Angulo et al. 1999). Though these resonances have been the subject of several direct experimental investigations (Mak et al. 1978; Lorentz-Wirzba et al. 1979) as well as of many spectroscopic studies (Yagi et al. 1962; Champagne & Pitt 1986; Wiescher & Kettner 1980; Schmidt & Duhm 1970), the reaction rate for this process has a considerable uncertainty (Angulo et al. 1999). With regard to the 20 keV resonance, its strength is known only from spectroscopic measurements performed through the transfer reaction $^{18}\text{O}(^3\text{He}, d)^{19}\text{F}$ (Champagne & Pitt 1986) and the direct capture reaction $^{18}\text{O}(p, \gamma)^{19}\text{F}$ (Wiescher & Kettner 1980). Therefore the deduced reaction rate is affected by large and not-well-defined uncertainties, because the deduced strengths are strongly model dependent. In fact they rely on the optical model potentials adopted in the data analysis, and different set of potentials or of parameters, though giving a reasonable account of the experimental data, lead to the extraction of different spectroscopic factors. An additional important source of uncertainty on the reaction rate is connected with the determination of the resonance energy for this resonance (Champagne & Pitt 1986). The resonance at 143.5 keV is fairly well established (Lorentz-Wirzba et al. 1979). The broad resonance at 656 keV gives strong contribution both at low and high temperatures. The total width of this high energy resonance is badly known and, as a consequence, also its contribution to the reaction rate. Two sets of widths are present in the literature, namely Yagi et al. (1962) and Lorentz-Wirzba et al. (1979). To sum up, the uncertainties on nuclear physics inputs have made astrophysical predictions far from conclusive (Nollett, Busso, & Wasserburg 2003). As already discussed, in this paper we will focus on the

low-laying resonances, below about 200 keV. In this range an additional resonance at 90 keV in the $^{18}\text{O}(p, \alpha)^{15}\text{N}$ cross section, corresponding to the 8.084 MeV excited state in ^{19}F occurs. The influence of this level on the reaction rate is also established.

3 The Trojan horse method

Two main reasons make the direct measurement of the cross section of astrophysically relevant reaction not accurate or even impossible: on one hand the presence of the Coulomb barrier, exponentially suppressing the cross section at the lowest energies, on the other the presence of atomic electrons. As regards the Coulomb suppression, inside the Gamow energy window the cross section for reactions among charged particle drops well below 10^{-12} barn, thus making statistical accuracy and signal-to-noise ratio very poor. Even in the few cases where the measurement has been possible, especially in the case of light nuclei, thanks to improved techniques and underground laboratories (Fiorentini, Kavanagh, & Rolfs 1995), the presence of atomic electrons has prevented the access to the relevant information, that is the bare nucleus cross section. In fact atomic electrons screen the nuclear charges thus determining an enhancement of the cross section at the lowest energies, which is not related to nuclear physics (Assenbaum et al. 1987). Therefore the cross section at the energies relevant to astrophysics has to be extracted by means of extrapolation from higher energies, where the cross section is more easily measured. The extrapolation is worked out by means of R-matrix calculations (see, for instance, Barker (2002)) or, if no calculations are available, by means of simple polynomial fit. As a result large uncertainties can be introduced into the astrophysical models because of an incorrect estimate of the relevant reaction rates, as we have argued in the case of the $^{18}\text{O}(p, \alpha)^{15}\text{N}$ reaction.

In order to reduce the nuclear uncertainties affecting its reaction rate we have performed an experimental study of the $^{18}\text{O}(p, \alpha)^{15}\text{N}$ reaction by means of the Trojan horse method (THM), which is an indirect technique to measure the relative energy-dependence of a charged-particle reaction cross section at energies well below the Coulomb barrier (La Cognata et al. (2007); Spitaleri et al. (1999) and references therein). The cross section of the $^{18}\text{O}(p, \alpha)^{15}\text{N}$ reaction is deduced from the $^2\text{H}(^{18}\text{O}, \alpha^{15}\text{N})n$ three-body process, performed in quasi-free (QF) kinematics. The beam energy is chosen larger than the Coulomb barrier of the interacting nuclei, so the break-up of the deuteron (acting as the *Trojan-horse* nucleus) takes place inside the ^{18}O nuclear field. Therefore, the cross section of the $^{18}\text{O}(p, \alpha)^{15}\text{N}$ reaction is not suppressed by the Coulomb interaction of the target-projectile system, while no electron screening enhancement is spoiling the nuclear information because the reaction is performed at high energies (several tens of MeV). The QF reaction mechanism for the $^2\text{H}(^{18}\text{O}, \alpha^{15}\text{N})n$ process is sketched in Fig. 1.

The THM cross section for the $^{18}\text{O} + d(p \oplus n) \rightarrow ^{15}\text{N} + \alpha + n$ reaction proceeding through a resonance

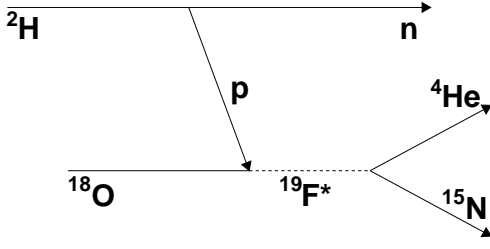


Figure 1: Simple sketch of the ${}^2\text{H}({}^{18}\text{O}, \alpha{}^{15}\text{N})n$ TH reaction.

${}^{19}\text{F}_i$ in the subsystem ${}^{19}\text{F} = {}^{18}\text{O} + p = {}^{15}\text{N} + \alpha$ can be obtained if the process is described as a transfer to the continuum, where the emitted neutron keeps the same momentum as the one it has inside deuteron (QF condition). If such a hypothesis is satisfied, the cross section for the QF ${}^2\text{H}({}^{18}\text{O}, \alpha{}^{15}\text{N})n$ three-body reaction is (La Cognata et al. 2007; Mukhamedzhanov et al. 2008)

$$\frac{d^2\sigma}{dE_{\alpha{}^{15}\text{N}} d\Omega_n} \propto \frac{\Gamma_{(\alpha{}^{15}\text{N})_i}(E) |M_i(E)|^2}{(E - E_{R_i})^2 + \Gamma_i^2(E)/4}. \quad (1)$$

Here, $M_i(E)$ is the direct transfer reaction amplitude for the binary reaction ${}^{18}\text{O} + d \rightarrow {}^{19}\text{F}_i + n$ leading to the population of the i -th resonant state of ${}^{19}\text{F}$ with the resonance energy E_{R_i} , E is the ${}^{18}\text{O} - p$ relative kinetic energy related to $E_{15\text{N}-\alpha}$ by the energy conservation law, $\Gamma_{(\alpha{}^{15}\text{N})_i}(E)$ is the partial resonance width for the decay ${}^{19}\text{F}_i \rightarrow \alpha - {}^{15}\text{N}$ and Γ_i is the total resonance width of ${}^{19}\text{F}_i$. The appearance of the transfer reaction amplitude $M_i(E)$ instead of the entry channel partial resonance width $\Gamma_{(p{}^{18}\text{O})_i}(E)$ is the main difference between the THM cross section and the cross section for the resonant binary sub-reaction ${}^{18}\text{O} + p \rightarrow {}^{15}\text{N} + \alpha$ (La Cognata et al. 2007; Mukhamedzhanov et al. 2008). Therefore the cross section of the three-body process can be easily connected to the one for the two-body reaction of interest by evaluating the transfer amplitude $M_i(E)$. In the plane wave approximation $M_i \approx \varphi_d(p_{pn}) W_{p{}^{18}\text{O}}(\mathbf{p}_{p{}^{18}\text{O}})$, where $\varphi_d(p_{pn})$ is the Fourier transform of the s -wave radial $p - n$ bound-state wave function, p_{pn} is the $p - n$ relative momentum, and $W_{p{}^{18}\text{O}}(\mathbf{p}_{p{}^{18}\text{O}})$ is the form factor for the synthesis ${}^{18}\text{O} + p \rightarrow {}^{19}\text{F}_i$ (La Cognata et al. 2007, 2008). In the present case no distortion are observed because of the high beam energy and because the emitted neutron in the exit channel has no long range Coulomb interaction.

4 Experimental investigation

The experiment was performed at Laboratori Nazionali del Sud, Catania (Italy) and represents the continuation of the one carried out at the Cyclotron Institute, Texas A&M University, Texas (USA). The SMP Tandem Van de Graaff accelerator provided the 54

MeV ${}^{18}\text{O}$ beam which was accurately collimated to achieve the best angular resolution. The intensity was 5 nA on the average and the relative beam energy spread was about 10^{-4} . Thin self-supported deuterated polyethylene (CD₂) targets, about $100 \mu\text{g}/\text{cm}^2$ thick, were adopted in order to minimize angular straggling. The detection setup consisted of a telescope (A), to single out $Z=7$ particles, made up of an ionization chamber and a silicon position sensitive detector (PSD A). Negligible angular straggling was introduced on the ${}^{15}\text{N}$ detection by the ionization chamber. Three additional silicon PSD's (B, C and D) were placed on the opposite side, with the aim of detecting alpha particles from the ${}^2\text{H}({}^{18}\text{O}, \alpha{}^{15}\text{N})n$ QF three-body process. No ΔE detectors were put in front of PSD's B, C and D to decrease detection thresholds and to achieve the best energy and angular resolution. Angular conditions were selected in order to maximize the expected QF contribution.

A description of the data analysis is reported in La Cognata et al. (2008), here we shortly summarize the main stages. After detector calibration, the first step of the analysis was the reaction channel selection. This is necessary because several reactions can take place in the target, while only partial particle identification is allowed by the experimental setup. In detail, α -particle identification as well as $A=15$ selection in PSD A were accomplished from the kinematics of the events. Indeed in a three-body reactions the events gather in some well-defined kinematical regions, fixed by the Q-value of the three-body process. The procedure discussed in Costanzo et al. (1990) was then applied after gating on the time-to-amplitude converter to select the coincidence peak and on the $\Delta E - E$ 2D spectra to select the nitrogen locus. The kinematic locus of the ${}^2\text{H}({}^{18}\text{O}, \alpha{}^{15}\text{N})n$ reaction was then extracted and compared to the corresponding one, obtained by means of a Monte Carlo simulation, showing that no additional channels contribute to the experimental kinematic locus.

A further study on reaction dynamics is necessary to select those kinematic regions where QF break-up is dominant and can be separated from direct break-up (DBU) or sequential decay (SD). To this purpose the $E_{15\text{N}-n}$ and the $E_{\alpha-n}$ relative energy spectra were extracted to evaluate the contribution from ${}^{16}\text{N}^*$ and ${}^5\text{He}^*$ excited states. On the other hand, since the same resonances in the the ${}^{19}\text{F}^* + n$ channel can be observed through QF and SD reaction mechanisms, the experimental neutron momentum distribution has been evaluated. Indeed, only if the deuteron break-up process is direct the neutron momentum distribution keeps the same shape as inside d . The procedure to extract the experimental neutron momentum distribution is extensively discussed in La Cognata et al. (2007) and Spitaleri et al. (2004). The resulting distribution is compared with the theoretical one given by the square of the Hulthén wave function in momentum space (La Cognata et al. 2007; Spitaleri et al. 2004). The good agreement demonstrates that the QF mechanism is present and dominant in the $p_3 < 50 \text{ MeV}/c$ neutron momentum range. In addition, inside this region the contribution from the SD of ${}^{16}\text{N}$ excited states

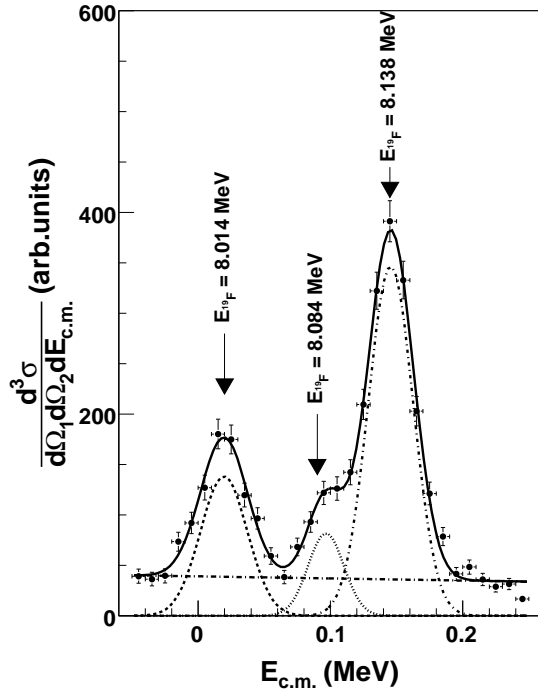


Figure 2: Cross section of the ${}^2\text{H}({}^{18}\text{O}, \alpha{}^{15}\text{N})n$ TH reaction. See text for details.

is negligible. For these reasons, in the following analysis only the phase space region for which the $p_3 < 50$ MeV/c condition is satisfied is taken into account.

The extracted three-body cross section has been integrated in the whole angular range. The resulting ${}^2\text{H}({}^{18}\text{O}, \alpha{}^{15}\text{N})n$ reaction cross section is shown in Fig. 2 (full circles). The experimental energy resolution turned out to be about 40 keV (FWHM). Horizontal error bars represent the integration bin while the vertical ones arise from statistical uncertainty and angular distribution integration. The solid line in the figure is the sum of three Gaussian functions to fit the resonant behavior and a straight line to account for the non-resonant contribution to the cross section. The resonance energies were then deduced: $E_{R_1} = 19.5 \pm 1.1$ keV, $E_{R_2} = 96.6 \pm 2.2$ keV and $E_{R_3} = 145.5 \pm 0.6$ keV (in fair agreement with the ones reported in the literature (Angulo et al. 1999)) as well as the peak values of each resonance in arbitrary units: $N_1 = 138 \pm 8$, $N_2 = 82 \pm 9$ and $N_3 = 347 \pm 8$. The peak values were used to derive the resonance strengths:

$$(\omega\gamma)_i = \frac{2J_{19F_i} + 1}{(2J_{18O} + 1)(2J_p + 1)} \frac{\Gamma_{(p^{18O})_i} \Gamma_{(\alpha^{15N})_i}}{\Gamma_i}, \quad (2)$$

that are the relevant parameters for astrophysical application in the case of narrow resonances (Angulo et al. 1999). The peak THM cross section taken at the E_{R_i} resonance energy for the (p, α) reaction $A + x \rightarrow C + c$ is given by

$$N_i = 4 \frac{\Gamma_{\alpha_i}(E_{R_i}) M_i^2(E_{R_i})}{\Gamma_i^2(E_{R_i})}, \quad (3)$$

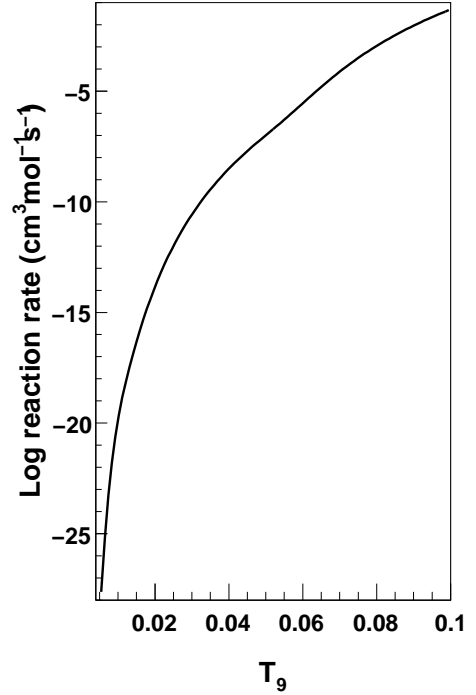


Figure 3: Reaction rate of the ${}^{18}\text{O}(p, \alpha){}^{15}\text{N}$ reaction.

where $\Gamma_{(\alpha^{15N})_i}(E) \equiv \Gamma_{\alpha_i}(E)$. In this work we did not extract the absolute value of the cross section. Anyway the proton and alpha partial widths for the third resonance are well known (Angulo et al. 1999), thus we can determine the strength for the 20 keV and 90 keV resonances from the ratio of the peak values of the THM cross sections, as discussed by La Cognata et al. (2008). The electron screening gives a negligible contribution around 144 keV (4% maximum (Assenbaum et al. 1987)), thus no systematic uncertainty is introduced by normalizing to the highest energy resonance. If $(\omega\gamma)_3$ is taken from Becker et al. (1995), one gets $(\omega\gamma)_1 = 8.3^{+3.8}_{-2.6} \times 10^{-19}$ eV, which is well within the confidence range established by NACRE, $6^{+17}_{-5} \times 10^{-19}$ eV (Angulo et al. 1999). This is because NACRE recommended value is based on spectroscopic data while the present result is obtained from experimental ones, thus increasing the accuracy of the deduced resonance strength. The largest contribution to the error is due to the uncertainty on the resonance energy, while statistical and normalization errors sum up to about 9.5%. To cross check the method, we have extracted the resonance strength of the 90 keV resonance, which is known with fairly good accuracy $((1.6 \pm 0.5) \times 10^{-7}$ eV (Angulo et al. 1999)). We got $(\omega\gamma)_2 = (1.76 \pm 0.33) \times 10^{-7}$ eV (statistical and normalization errors $\sim 13\%$), in good agreement with the strength given by NACRE, giving us confidence in the theory used in the present paper.

5 Extraction of the reaction rate

By using the narrow resonance approximation (Angulo et al. 1999), which is fulfilled for the resonances under investigation, the reaction rate for the $^{18}\text{O}(p, \alpha)^{15}\text{N}$ reaction has been deduced. According to this approximation, the contribution to the rate of the i -th resonance is given by:

$$N_A \langle \sigma v \rangle_{R_i} = N_A \left(\frac{2\pi}{\mu k_B} \right)^{3/2} \hbar^2 (\omega\gamma)_i T^{-3/2} \exp(-E_{R_i}/k_B T) \quad (4)$$

where μ is the reduced mass for the projectile-target system and T is the temperature of the astrophysical site. The resulting rate $R_{^{18}\text{O}(p, \alpha)^{15}\text{N}}$ is displayed, as a function of the temperature, in Fig. 3. The analytic expression of the reaction rate (with $\approx 10\%$ accuracy) is:

$$R_{^{18}\text{O}(p, \alpha)^{15}\text{N}} = \frac{5.58 \cdot 10^{11}}{T_9^{2/3}} \exp\left(-\frac{16.732}{T_9^{1/3}} - \left(\frac{T_9}{0.51}\right)^2\right) + \frac{1.375 \cdot 10^{-13}}{T_9^{3/2}} \exp\left(-\frac{0.232}{T_9}\right) + \frac{2.58 \cdot 10^4}{T_9^{3/2}} \exp\left(-\frac{1.665}{T_9}\right) + \frac{3.24 \cdot 10^8}{T_9^{0.378}} \exp\left(-\frac{6.395}{T_9}\right) \quad (5)$$

where T_9 is the temperature in billion kelvin and the reaction rate $R_{^{18}\text{O}(p, \alpha)^{15}\text{N}}$ is measured in $\text{cm}^3 \text{mol}^{-1} \text{sec}^{-1}$. This expression is obtained by using as a fitting function a formula similar to the NACRE one, leaving as free parameters the numerical coefficients and using as initialization parameters the NACRE ones (Angulo et al. 1999).

Because of the strong dependence on the temperature (for a factor 10 change in the temperature, the reaction rate increases by about 30 orders of magnitude), any comparison of the present results with the one in the literature is very difficult. In order to compare with the one reported in NACRE (Angulo et al. 1999), the ratio of the THM reaction rate to the NACRE one for the $^{18}\text{O}(p, \alpha)^{15}\text{N}$ reaction is shown as a full black line in Fig. 4. In this representation, the NACRE rate is given by a full red line, that is by 1 in the whole examined range. The dot-dashed and dotted black lines represent the upper and lower limits respectively, allowed by the experimental uncertainties. As before, black and red lines mark THM and NACRE data. In the low temperature region (below $T_9 = 0.03$, Fig. 4a) the reaction rate can be about 35% larger than the one given by NACRE, while the indetermination is greatly reduced with respect to the NACRE one, by a factor ≈ 8.5 , in the case the error on the NACRE rate is supposed to come entirely from the uncertainty on the 20 keV resonance strength, to make the comparison homogenous. Those temperatures are typical of the bottom of the convective envelope, thus an increase of this reaction rate might

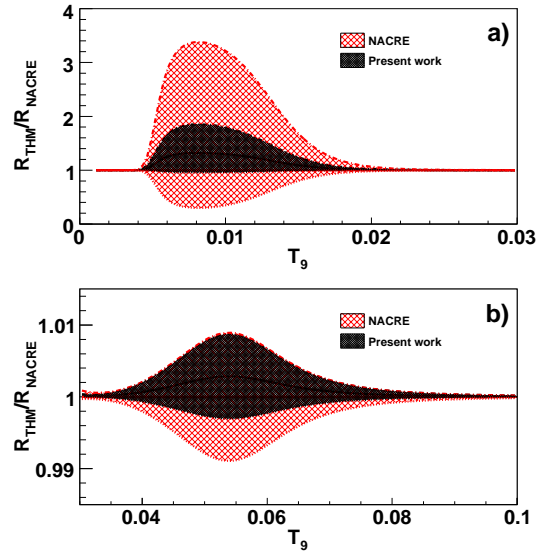


Figure 4: Comparison of the reaction rate of the $^{18}\text{O}(p, \alpha)^{15}\text{N}$ reaction with the NACRE one (Angulo et al. 1999).

have important consequences on the cool bottom process (Nollett, Busso, & Wasserburg 2003) and, in turn, on the surface abundances and isotopic ratios in AGB stars. The 8.084 MeV excited state of ^{19}F (corresponding to the 90 keV resonance) provides a negligible contribution to the reaction rate in agreement with the previous estimate by Champagne & Pitt (1986). This is clearly displayed by Fig. 4b), where an increase of less than 1% is obtained due to the THM measurement of the 90 keV level resonance strength. For completeness, the THM reaction rate and the NACRE one are given in Tab. 1, together with the upper and lower limits allowed by experimental uncertainties. As discussed before, the confidence range for the NACRE rate is evaluated by assuming that the only source of indetermination is coming from the 20 keV resonance, to make the comparison meaningful.

6 Final remarks

In this paper we have evaluated the influence of the new improved measurement of the 20 keV resonance on the reaction rate of the $^{18}\text{O}(p, \alpha)^{15}\text{N}$ reaction. In fact, for the first time, the strength of the low-lying 20 keV resonance in ^{19}F has been experimentally determined thanks to the use of the indirect THM, while the same measurements have been proved elusive for any direct approach (see La Cognata et al. (2008) for a detailed discussion). The present result turns out to be about 35% larger than the NACRE rate (Angulo et al. 1999) in the region where the effect of the presence of the 20 keV resonance is more intense. This newly developed approach, which is based on experimental data in contrast to the NACRE one that relies on various kinds of estimates, has allowed to enhance the accu-

Table 1: Rate of the $^{18}\text{O}(p, \alpha)^{15}\text{N}$ reaction, in comparison with the one from NACRE (Angulo et al. 1999)

Temperature (10^9 K)	Rate THM ($\text{cm}^3\text{mol}^{-1}\text{s}^{-1}$)			Rate NACRE ($\text{cm}^3\text{mol}^{-1}\text{s}^{-1}$)		
	lower	adopted	upper	lower	adopted	upper
0.007	$8.12 \cdot 10^{-25}$	$1.11 \cdot 10^{-24}$	$1.54 \cdot 10^{-24}$	$2.75 \cdot 10^{-25}$	$8.44 \cdot 10^{-25}$	$2.78 \cdot 10^{-24}$
0.008	$4.02 \cdot 10^{-23}$	$5.55 \cdot 10^{-23}$	$7.79 \cdot 10^{-23}$	$1.25 \cdot 10^{-23}$	$4.19 \cdot 10^{-23}$	$1.42 \cdot 10^{-22}$
0.009	$8.60 \cdot 10^{-22}$	$1.18 \cdot 10^{-21}$	$1.65 \cdot 10^{-21}$	$2.78 \cdot 10^{-22}$	$8.95 \cdot 10^{-22}$	$2.99 \cdot 10^{-21}$
0.010	$1.03 \cdot 10^{-20}$	$1.39 \cdot 10^{-20}$	$1.92 \cdot 10^{-20}$	$3.71 \cdot 10^{-21}$	$1.06 \cdot 10^{-20}$	$3.42 \cdot 10^{-20}$
0.011	$8.15 \cdot 10^{-20}$	$1.07 \cdot 10^{-19}$	$1.45 \cdot 10^{-19}$	$3.47 \cdot 10^{-20}$	$8.43 \cdot 10^{-20}$	$2.53 \cdot 10^{-19}$
0.012	$4.90 \cdot 10^{-19}$	$6.22 \cdot 10^{-19}$	$8.14 \cdot 10^{-19}$	$2.52 \cdot 10^{-19}$	$5.04 \cdot 10^{-19}$	$1.36 \cdot 10^{-18}$
0.013	$2.45 \cdot 10^{-18}$	$2.96 \cdot 10^{-18}$	$3.72 \cdot 10^{-18}$	$1.51 \cdot 10^{-18}$	$2.50 \cdot 10^{-18}$	$5.87 \cdot 10^{-18}$
0.014	$1.07 \cdot 10^{-17}$	$1.24 \cdot 10^{-17}$	$1.48 \cdot 10^{-17}$	$7.76 \cdot 10^{-18}$	$1.09 \cdot 10^{-17}$	$2.17 \cdot 10^{-17}$
0.015	$4.30 \cdot 10^{-17}$	$4.75 \cdot 10^{-17}$	$5.40 \cdot 10^{-17}$	$3.48 \cdot 10^{-17}$	$4.35 \cdot 10^{-17}$	$7.28 \cdot 10^{-17}$
0.016	$1.58 \cdot 10^{-16}$	$1.69 \cdot 10^{-16}$	$1.85 \cdot 10^{-16}$	$1.39 \cdot 10^{-16}$	$1.60 \cdot 10^{-16}$	$2.30 \cdot 10^{-16}$
0.018	$1.72 \cdot 10^{-15}$	$1.76 \cdot 10^{-15}$	$1.83 \cdot 10^{-15}$	$1.64 \cdot 10^{-15}$	$1.72 \cdot 10^{-15}$	$2.02 \cdot 10^{-15}$
0.020	$1.41 \cdot 10^{-14}$	$1.42 \cdot 10^{-14}$	$1.44 \cdot 10^{-14}$	$1.38 \cdot 10^{-14}$	$1.41 \cdot 10^{-14}$	$1.50 \cdot 10^{-14}$
0.025	$1.00 \cdot 10^{-12}$	$1.01 \cdot 10^{-12}$	$1.01 \cdot 10^{-12}$	$1.00 \cdot 10^{-12}$	$1.00 \cdot 10^{-12}$	$1.01 \cdot 10^{-12}$
0.030	$2.64 \cdot 10^{-11}$	$2.64 \cdot 10^{-11}$	$2.64 \cdot 10^{-11}$	$2.64 \cdot 10^{-11}$	$2.64 \cdot 10^{-11}$	$2.64 \cdot 10^{-11}$
0.040	$3.12 \cdot 10^{-9}$	$3.12 \cdot 10^{-9}$	$3.12 \cdot 10^{-9}$	$3.12 \cdot 10^{-9}$	$3.12 \cdot 10^{-9}$	$3.12 \cdot 10^{-9}$
0.050	$1.01 \cdot 10^{-7}$	$1.01 \cdot 10^{-7}$	$1.01 \cdot 10^{-7}$	$1.01 \cdot 10^{-7}$	$1.01 \cdot 10^{-7}$	$1.01 \cdot 10^{-7}$
0.060	$2.81 \cdot 10^{-6}$	$2.81 \cdot 10^{-6}$	$2.81 \cdot 10^{-6}$	$2.81 \cdot 10^{-6}$	$2.81 \cdot 10^{-6}$	$2.81 \cdot 10^{-6}$
0.070	$7.52 \cdot 10^{-5}$	$7.52 \cdot 10^{-5}$	$7.52 \cdot 10^{-5}$	$7.52 \cdot 10^{-5}$	$7.52 \cdot 10^{-5}$	$7.52 \cdot 10^{-5}$
0.080	$1.10 \cdot 10^{-3}$	$1.10 \cdot 10^{-3}$	$1.10 \cdot 10^{-3}$	$1.10 \cdot 10^{-3}$	$1.10 \cdot 10^{-3}$	$1.10 \cdot 10^{-3}$
0.090	$9.07 \cdot 10^{-3}$	$9.07 \cdot 10^{-3}$	$9.07 \cdot 10^{-3}$	$9.07 \cdot 10^{-3}$	$9.07 \cdot 10^{-3}$	$9.07 \cdot 10^{-3}$
0.100	$4.88 \cdot 10^{-2}$	$4.88 \cdot 10^{-2}$	$4.88 \cdot 10^{-2}$	$4.88 \cdot 10^{-2}$	$4.88 \cdot 10^{-2}$	$4.88 \cdot 10^{-2}$

racy of the rate, reducing the uncertainty due to the poor knowledge of the parameters of the 20 keV resonance in the $^{18}\text{O}(p, \alpha)^{15}\text{N}$ reaction by a factor ≈ 8.5 . Such a remarkable improvement is mainly due to two reasons. On one hand, the THM bring to the determination of the strength of the unknown resonance avoiding information about the spectroscopic factors, which are a primary source of systematic errors. On the other, our results are not affected by the electron screening, which can enhance the cross section by a factor larger than about 2.4 at 20 keV (Assenbaum et al. 1987), thus spoiling any direct measurement of this resonance. As a next step, the astrophysical consequences of the present work are to be evaluated, both onto the scenarios sketched in the introduction and on alternative environments. In addition, at higher temperatures, higher energy resonances in the $^{18}\text{O}(p, \alpha)^{15}\text{N}$ reaction can play a role. These studies will be the subject of forthcoming works.

References

- Renda, A., et al. 2004, MNRAS, 354, 575
- Jorissen, A., Smith, V. V., & Lambert, D. L. 1992, A&A, 261, 164
- Lugaro, M., et al. 2004, ApJ, 615, 934
- Nollett, K. M., Busso, M., & Wasserburg, G. J. 2003, ApJ, 582, 1036
- Angulo, C., et al. 1999, NPA, 656, 3
- Mak, H.B., et al., 1978, NPA, 304, 210
- Lorentz-Wirzba, H., et al., 1979, NPA, 313, 346
- Yagi, K., et al., 1962, J. Phys. Soc. Japan, 17, 595
- Champagne, A.E., & Pitt, M., 1986, NPA, 457, 367
- Wiescher, M., & Kettner, K.U., 1980, NPA, 349, 165
- Schmidt, C., & Duhm, H.H., 1970, NPA, 155, 644
- Fiorentini, G., Kavanagh, R.W., & Rolfs, C., 1995, Z. Phys. A, 350, 289
- Barker, F.C., 2002, NPA 707, 277
- Spitaleri, C., et al., 1999, PRC, 60, 055802
- La Cognata, M., et al., 2007, PRC, 76, 065804
- Mukhamedzhanov, A.M., et al., 2008 J. Phys. G: Nucl. Part. Phys., 35, 014016
- Assenbaum, H.J., et al., 1987, Z. Phys. A, 327, 461
- La Cognata, M., et al., 2008, PRL, 101, 152501
- Costanzo, E., et al., 1990, NIM A, 295, 373
- Spitaleri, C., et al., 2004, PRC, 69, 055806
- Becker, H.W., et al., 1995, Z. Phys. A, 351, 453